

Geophysical Research Letters

RESEARCH LETTER

10.1029/2019GL083601

Key Points:

- In the Ganges-Brahmaputra-Meghna Delta, the Indian Craton, and the Indo-Burman subduction zone enhance the subsidence due to sediment loading toward the east
- The subsidence rate estimates (2–3 mm/year) are comparable to the present-day global mean sea level rise
- Subsidence rates are maximum in the most populated area of the delta

Supporting Information:

- Supporting Information S1
- Figure S1
- Figure S2
- Figure S3

Correspondence to:

Y. Krien,
ykrien@gmail.com

Citation:

Krien, Y., Karpytchev, M., Ballu, V., Becker, M., Grall, C., Goodbred, S., et al. (2019). Present-day subsidence in the Ganges-Brahmaputra-Meghna Delta: Eastern amplification of the Holocene sediment loading contribution. *Geophysical Research Letters*, 46, e2019GL083601. <https://doi.org/10.1029/2019GL083601>

Received 5 MAY 2019

Accepted 3 SEP 2019

Accepted article online 11 SEP 2019

Published online 10 OCT 2019

Present-Day Subsidence in the Ganges-Brahmaputra-Meghna Delta: Eastern Amplification of the Holocene Sediment Loading Contribution

Y. Krien^{1,2}, M. Karpytchev², V. Ballu², M. Becker², C. Grall³, S. Goodbred⁴, S. Calmant⁵, C. K. Shum^{6,7}, and Z. Khan⁸

¹LARGE, University of the French West Indies, Guadeloupe, France, ²LIENSs, UMR 7266 CNRS, University of La Rochelle, La Rochelle, France, ³Lamont-Doherty Earth Observatory, Columbia University, New York, NY, USA,

⁴Department of Earth and Environmental Sciences, Vanderbilt University, Nashville, TN, USA, ⁵LEGOS,

UMR5566/CNRS/CNES/IRD/UPS, University of Toulouse III, Toulouse, France, ⁶Division of Geodetic Science, School of Earth Sciences, Ohio State University, Columbus, OH, USA, ⁷Institute of Geodesy and Geophysics, Chinese Academy of Sciences, Wuhan, China, ⁸Institute of Water Modelling, Dhaka, Bangladesh

Abstract The subsidence of the Ganges-Brahmaputra-Meghna Delta (GBMD) drastically increases the adverse impacts of coastal flooding and exacerbates the vulnerability of populations from ongoing rapid sea level rise. We focus here on estimating the present-day subsidence rates induced by the loading of sediments continuously deposited within the GBMD over the past 11,000 years. By constructing a realistic GBMD 3-D numerical model with laterally variable mantle and lithospheric structure, we demonstrate for the first time that the presence of the strong Indian Craton and the weakened Indo-Burma margin results in significant amplification of subsidence driven by sediment loading in the eastern part of the delta, where the population density is the highest (>1,000 habitants per km²). Although uncertainties remain regarding the amplitude of subsidence, the rate estimates (2–3 mm/year) are found to be comparable to the present-day global mean sea level rise.

Plain Language Summary Using 3-D numerical models, we show that the deformation of the Earth surface due to the weight of sediments deposited in the Ganges-Brahmaputra-Meghna Delta (GBMD) is probably larger than previously found and induce significant land vertical downward motions in the eastern part of the delta. This process is intimately linked to the complex geological setting of the GBMD (Indian Craton, tectonic plate boundaries), which enhances vertical velocities toward the east. The maximum velocities are found to be located in the region where the population density is the highest. They are of the same order as the rates of present-day global mean sea level rise.

1. Introduction

For thousands of years, a large number of people have been attracted by the rich fertile plains of the Ganges-Brahmaputra-Meghna Delta (GBMD). The GBMD (Figure 1) is today one of the world's most densely populated regions (>1,000 habitants per km²; WorldPop, 2017) and one of the most vulnerable ones (Milliman et al., 1989). With about 150 million people living just a few meters above mean sea level (Higgins, 2016), the GBMD is particularly exposed to severe cyclones, storm surges, river flooding, salinity intrusion, and coastal erosion (Chiu & Small, 2016). The devastating consequences of extreme events have raised deep concerns regarding the impact of climate change in the near future (Broadus et al., 1986, Milliman et al., 1989, Syvitski et al., 2009).

As in most deltas (Syvitski et al., 2009), land subsidence in the GBMD largely contributes to the steep relative sea level rise (Brown & Nicholls, 2015). Measurements of the present-day subsidence rates remain challenging as vertical displacements reflect various processes (such as sediment loading, sediment compaction, groundwater withdrawal, or tectonics) operating at different temporal and spatial scales. Within a relatively limited area of about 104 km² around Dhaka, InSAR (Interferometric Synthetic Aperture Radar) observations over a 5-year period (2007–2011) revealed, for instance, subsidence rates varying from 0 to as much as 18 mm/year (Higgins et al., 2014). A similar range of rates (between 0 and 13 mm/year) was reported by preliminary GPS analysis throughout the delta over a longer period (e.g., Steckler et al., 2013). Further work is in progress, however, to ensure that subsidence is properly captured using this method.

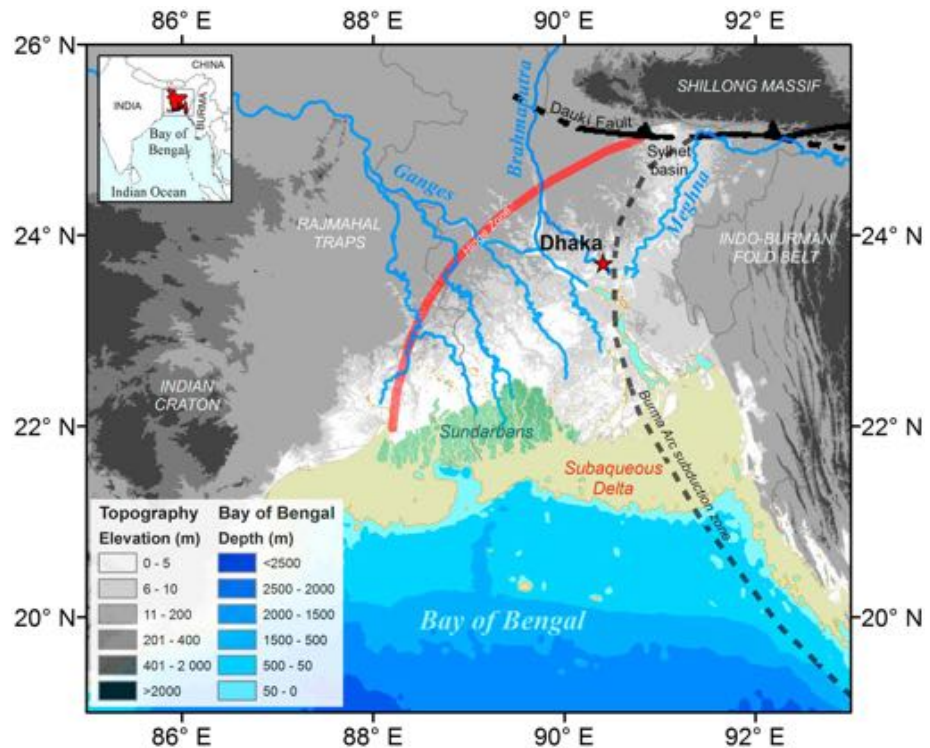


Figure 1. The Ganges-Brahmaputra-Meghna Delta (GBMD). The Hinge Zone (red line) represents the position of the Eocene shelf edge, as well as the eastern limit of the Indian Craton. The deformation front (dashed black line) is adapted from Steckler et al. (2008) and Grall et al. (2018). The subaqueous delta (0–20-m depth) and mangrove area (the Sundarbans) are depicted in brown and green, respectively.

Recently, a millennial-scale map of subsidence has been proposed by Grall et al. (2018). This work relies on a broad data set of stratigraphic data and revealed that the Holocene subsidence gradually increases from the Hinge Zone (Figure 1) to the southeastern edge of the delta, where it reaches about 5 mm/year. These results are in agreement with a number of previous studies (e.g., Hoque & Alam, 1997) and suggest that long-term processes such as sediment loading and compaction are major drivers of subsidence in the GBMD (Grall et al., 2018). Understanding the relative contribution of these processes thus appears to be particularly relevant.

Using a viscoelastic Earth model and sediment deposition history based on in situ measurements, Karpytchev et al. (2018) found that up to 1.6 mm/year of the present-day subsidence could be explained by Holocene sediment loading. Following previous studies, including Ivins et al. (2007), Wolstencroft et al. (2014), and Ferrier et al. (2015), they assumed that the Earth is laterally uniform. Such models, although useful in capturing sensitivity of the Earth surface displacements to variations of mantle viscosity with depth, fail to account for the effects of lateral variations in the lithospheric thickness and mantle viscosity due to continental cratons, fault systems, or mountain belts (Karpychev & Fleitout, 2000; Latychev et al., 2005; Spada et al., 2006). The assumption of a laterally uniform Earth is not expected to be adequate for the GBMD, whose geological setting is extremely complex. Indeed, the GBMD lies at the collision zone between two major tectonic plates: India and Eurasia. It is bounded by the Dauki fault system and the Shillong Massif to the north, the Indian Craton to the west, and the Indo-Burma foldbelt (a faulted and tectonically active area that incorporated the thick sediment piles from the Bengal Basin) to the east (Figure 1). These features probably explain to some extent the observed west-to-east decrease of flexural rigidity (Hammer et al., 2013) and are thus expected to play a key role in the response of the delta to sediment loading.

In this paper, we present the first 3-D numerical model of Holocene sediment loading in the GBMD (section 2). This model is used to investigate the impact of lateral rheological variations due to the Indian Craton and the weakened lithosphere of the Indo-Burman subduction zone and fold belt on sediment-driven subsidence rates (section 3). We will show that taking these lateral changes into account allows for

a better representation of the pattern of subsidence due to sediment loading and provides important insights into the processes driving the subsidence in the GBMD (section 4).

2. The Numerical Model

The response of the Earth to sediment loading is investigated using the finite element software for structural and fluid mechanics CAST3M (<http://www-cast3m.cea.fr/>), developed by the French Alternative Energies and Atomic Commission, which solves the governing equations of mass and momentum conservation for a wide variety of rheological properties.

We consider a portion of spherical shell representing the Earth, extending from the surface to 1,500-km depth, from 3°N to 43°N in latitude and from 70°E to 110°E in longitude (Figure 2a). This computational domain was found to be large enough to ensure that the results are only marginally dependent on the lateral boundary conditions. In particular, they do not vary if the size of the model is further increased.

The domain is discretized using six-nodes triangular prisms. The size of the elements varies in most cases from about 15 km in the GBMD and at plate boundaries to 200 km in the lower mantle near the limits of the domain (Figures 2a and 2c). The mesh is further refined (with resolutions up to 8 km) in cases for which the lithospheric thickness is reduced, to ensure that there are enough elements to properly capture the deformation of the plate. The mesh is generated by the software Gmsh (<http://gmsh.info>). It contains about 1.3 million elements in total in cases with a 80-km-thick lithosphere. Sensitivity tests were conducted to ensure that the results are only marginally dependent on the resolution and on the time step (10 years).

We hypothesize that the Earth deforms in response to loads as a Maxwell viscoelastic material (Peltier, 1974). The radial elastic properties are taken from the Preliminary Reference Earth Model (Dziewonski & Anderson, 1981). We consider the models composed of four layers: a rigid lithosphere with varying thickness, underlain by a weak asthenosphere, a stronger upper mantle in the transition zone (down to 670 km), and a viscous lower mantle.

The Indian Craton (Figure 2b) is represented as a thickened lithosphere underlain by a relatively strong asthenosphere, in agreement with tomographic images that reveal high seismic velocity anomalies in the upper mantle northwest of the Hinge Zone (Li et al., 2008). The location of plate margins is inferred from Steckler et al. (2008, 2010) and Grall et al. (2018). Since the structural geometry and deformation partitioning is highly complex east of the deformation front, several approaches were considered to incorporate these plate margins in the numerical model:

1. *A localized vertical plate boundary*: The plate boundary between the Indian Plate and Eurasia is represented by a 40-km-thick vertical layer with elements of reduced viscosity, extending from the surface down to the asthenosphere.
2. *A localized plate boundary with varying dip*: Same as in the previous case, but with a 30° dip of the weak layer in the eastern part of the delta (the area in dotted red in Figure 2b).
3. *A diffuse plate margin east of the delta*: In this approach, the viscosity of the lithosphere is less reduced than in previous cases, but over a larger area in the Indo-Burman foldbelt (area in red in Figure 2b).

The third case is likely to be more realistic for several reasons:

1. It is consistent with the fact that the plate convergence is accommodated (east of the GBMD) over a wide area, which extends from the deformation front to the internal part of the Indo-Burman Ranges (e.g., Steckler et al., 2016).
2. The shallowly dipping Indian Plate induces extremely large tectonic stresses in the overriding lithosphere, which is thus expected to be weakened over a wide area by a number of processes such as shear heating, dynamic recrystallization, fluid overpressure, advection of weak material into fault zones, or hydration/metamorphism (e.g., Tackley, 2000).
3. Diffuse weakened plate margins better reproduce the observed plate-like behavior (e.g., Zhong et al., 1998) and the gravity and geoid patterns (Krien & Fleitout, 2008) in subduction zone numerical models.

Sediment load histories for the past 11 kyr were extracted from the isopach map and sediment storage evolution provided by Goodbred & Kuehl, 2000a; Figure 3). Additional information on this work, as well as a sensitivity test on the impact of the loading history on the results, can be found in supporting information S1.

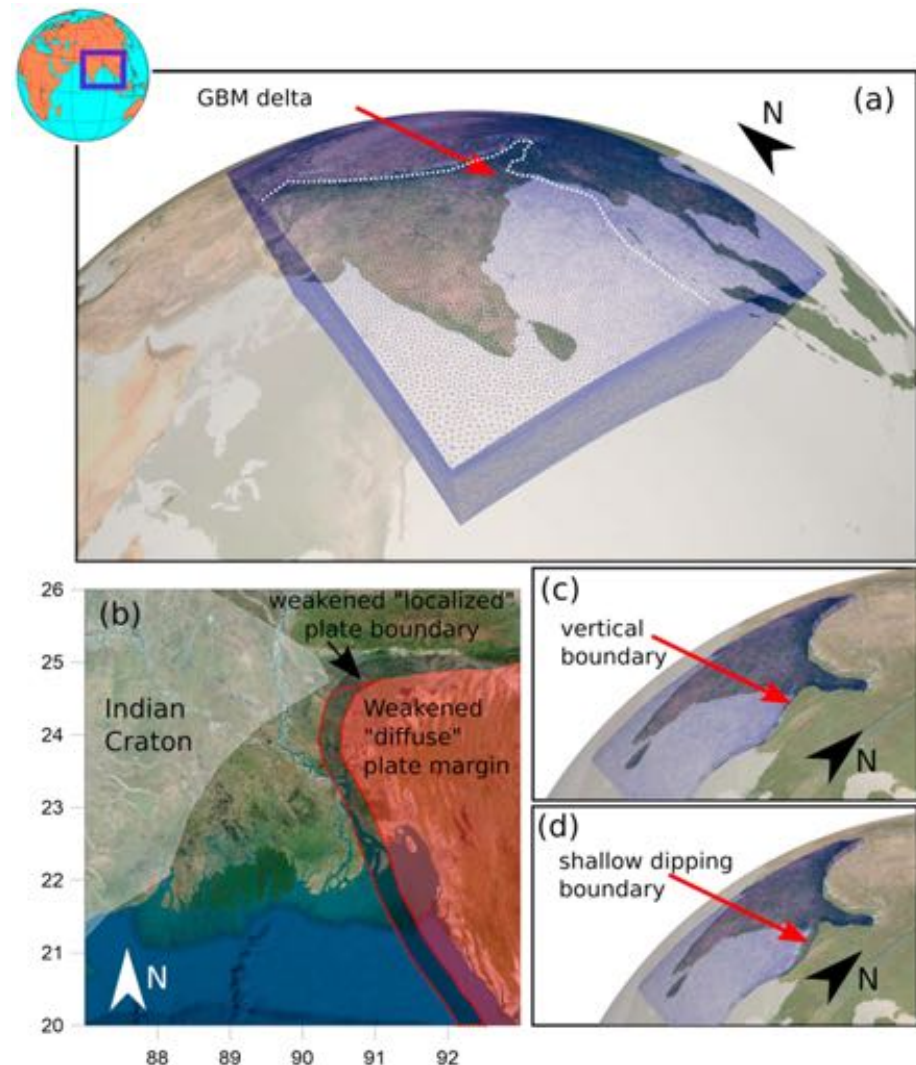


Figure 2. The 3-D numerical model. (a) Geographical extension of the computational domain. The approximate location of the plate boundary is depicted by the dashed white line; (b) location of the Indian Craton (in white), of the Indo-Burman subduction plate boundary when it is considered to be “localized” (in dark gray), and of the weakened part of the lithosphere when the plate margin is considered to be more diffuse (red + dotted red areas); (c) view of the mesh for the Indian lithosphere in the case of a vertical boundary; and (d) same for a shallow dipping boundary.

The effect of the eustatic sea level variations and sediment loading in the fan are neglected here, as they were found to have little impact on the subsidence in the delta.

Based on in situ measurements, a bulk density of $1,500 \text{ kg/m}^3$ is considered for sediments (Brammer, 1996; Goodbred & Kuehl, 2000a). We make the assumption that the shoreline was close to its present extent during the whole computation time. In practice, it means that

1. the subaqueous delta is under water. All the sediments deposited in this region displaced their own volume of water, so that only the difference between sediment and water density (500 kg/m^3) is accounted for,
2. and the floodplain is above sea level during the whole computation time (or was inundated only during very short periods of time). The full weight of sediments (density of $1,500 \text{ kg/m}^3$) is thus considered for this region.

The hypothesis for the subaqueous delta is rather conservative, as it was at least partially above mean sea level until about 9,000 cal year BP (Goodbred & Kuehl, 2000b). Our assumption is expected to be valid for

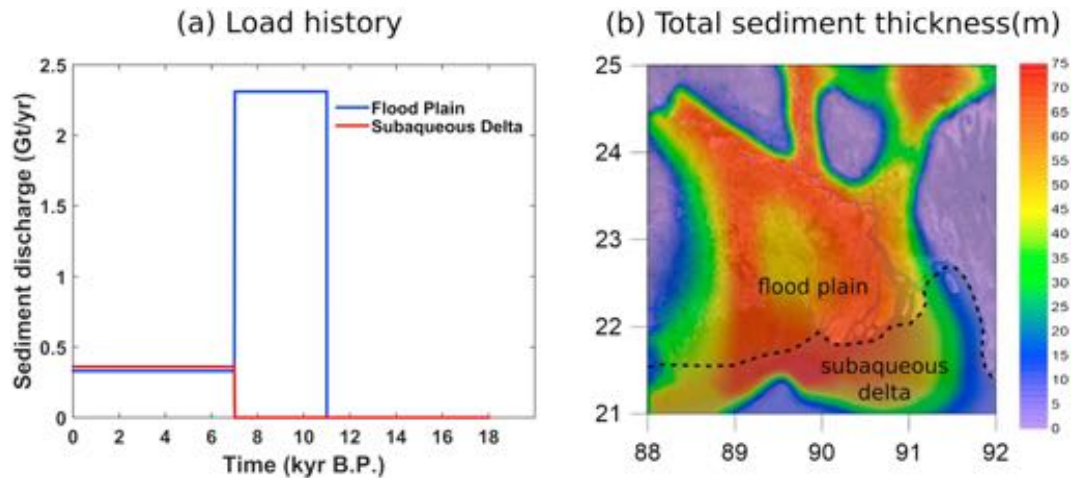


Figure 3. (a) Time history of sediment discharge (Gt/yr) on the GBMD flood plain (blue) and subaqueous delta (red). (b) Thickness (m) of Holocene sediments in the GBMD adapted from Goodbred and Kuehl (2000a). The dashed black line shows the boundary between the flood plain and the subaqueous delta.

the northern fluvial-dominated part of the delta, which was above mean sea level during Holocene (Grall et al., 2018). As for the southern tidal part of the deltaic plain, it was flooded only for a few hundreds of years around 6,500 year BC (Goodbred & Kuehl, 2000b; Rashid et al., 2013), due to a catastrophic meter-scale sea level rise (Blanchon & Shaw, 1995). For this short time period, our loading is thus expected to include a small part of the sea level rise contribution.

3. Results

Figure 4 displays the computed present-day vertical velocities due to sediment loading for different Earth structures. In case of a laterally uniform mantle, a nearly circular concentric pattern is found, with subsidence rates slightly higher than 1.5 mm/year for most of the deltaic plain (Figure 4a).

Introducing the Indian Craton as an area of thickened lithosphere and more viscous underlying mantle results in a much slower vertical movement within and close to the craton area (Figure 4b). These results are in agreement with the findings of Grall et al. (2018), who reported low subsidence rates (<0.5 mm/year) beyond the Hinge Zone, away from the delta plain. The subsidence map proposed by these authors is shown in supporting information S3. We find that the sediment-driven subsidence is now focused within a rather small region of the deltaic plain, with a slight shift of the maximum rates toward the southeast.

Incorporating a weak localized vertical plate boundary significantly changes the pattern of subsidence (Figure 4c). The vertical velocities are increased in the vicinity of the boundary, leading to a pattern of sediment-driven subsidence that is stretched northward, with a maximum of about 1.6 mm/year southeast of the delta, close to the mouth of Meghna. A more pronounced decrease of subsidence on the overriding plate is also observed. These features are less marked for a shallow dipping localized plate boundary (Figure 4d) but further amplified when the margin is represented as a larger and slightly stronger area (Figure 4e). In that case, the subsidence rates almost reach 2 mm/year along the Meghna and in the Sylhet Basin.

The results presented so far have been obtained using a relatively *hard mantle* hypothesis (Karpytchev et al., 2018). This assumption might be too conservative for the Bengal Basin, for which seismic observations suggest a rather weak mantle under the deltaic plain (Li et al., 2008). Following Karpytchev et al. (2018), an *intermediate* and a *soft mantle* hypothesis (with a 50- and 35-km-thick lithosphere, respectively, as well as a weaker mantle in the latter case) are thus also considered (Figures 4f and 4g). They lead to additional increase of subsidence rates, reaching 2.4 mm/year for the intermediate rheology and slightly more than 3.5 mm/year for the soft mantle hypothesis. More sensitivity tests were performed in supporting information S2, to investigate the impact of the uncertainty on the rheology. The *hard* and *soft* models shown

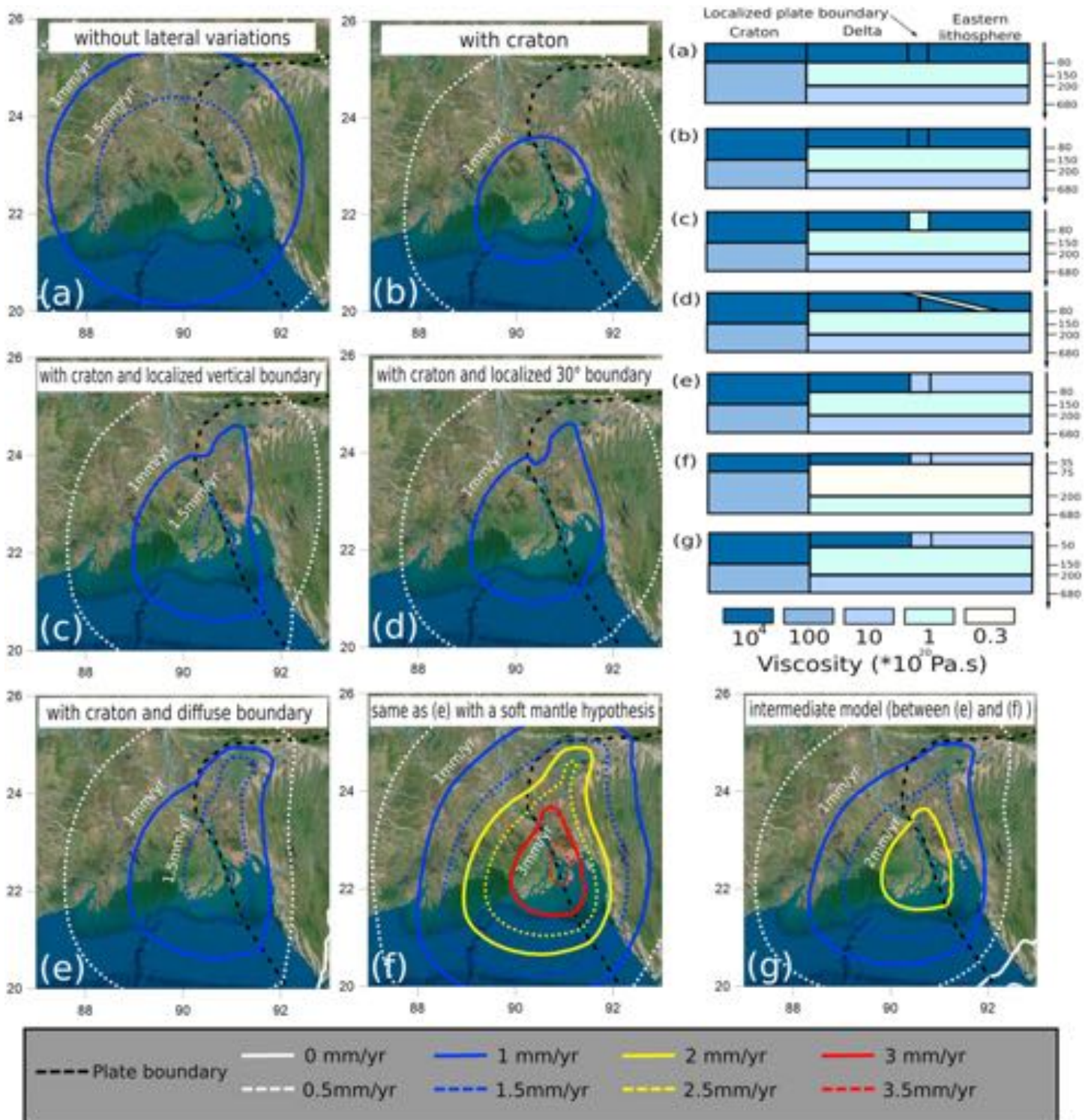


Figure 4. Computed present-day subsidence rates driven by sediment loading for different test cases. The dashed black curve represents the Indo-Burman subduction zone. The white, blue, yellow, and red solid lines give the isovalues of subsidence rates at 0, 1, 2, and 3 mm/year, respectively. The viscosity structure (from the surface to 670-km depth) is represented in each case along a west-to-east cross section. The vertical black lines divide up the different viscosity areas. The viscosity of the lower mantle is kept constant at 10^{22} Pa.s.

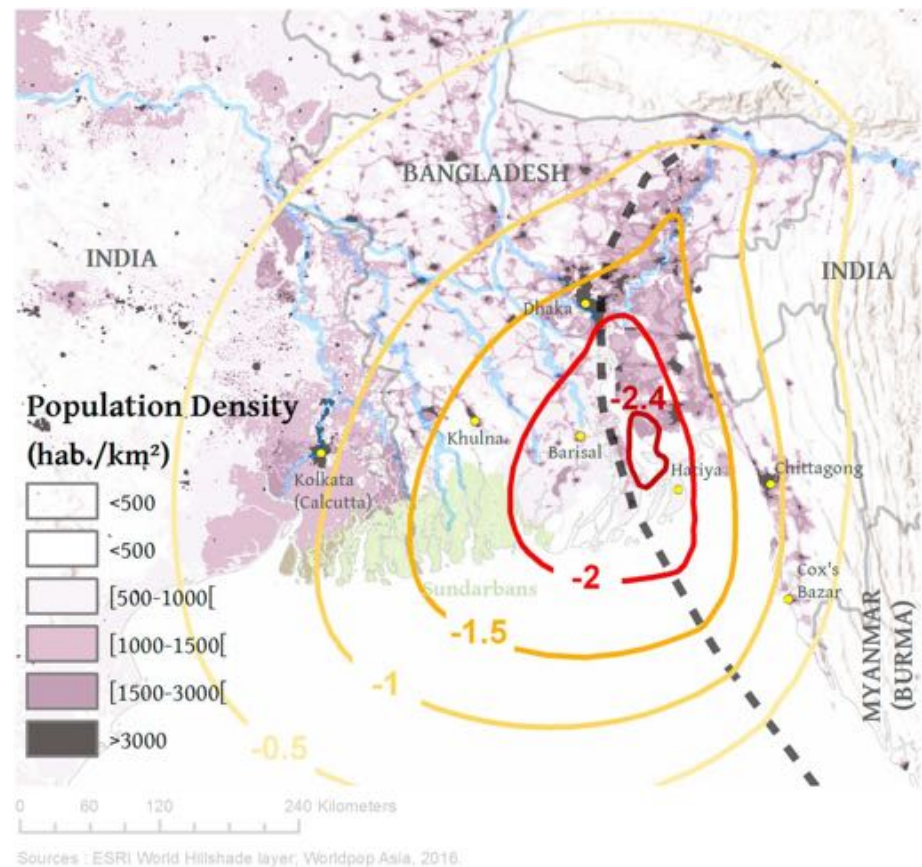


Figure 5. Population density in the GBMD. The contours represent the rates of sediment-driven subsidence for an intermediate model (model g in Figure 4).

in Figure 4 (cases [e] and [f], respectively) could be regarded as the lower and upper bounds of the response of GBMD to Holocene sediment loading.

4. Discussion and Conclusions

Using 3-D structural and fluid mechanics numerical models, we were able to start to unravel, for the first time, the implications of the complex geological setting of the GBMD on the pattern of subsidence. Including the strong Indian Craton and the weak Indo-Burman plate margin in the models leads indeed to a shifting of the sediment-driven subsidence toward the southeast, close to the Indian plate boundary. These features do not change when considering subsidence rates averaged over the Holocene (see supporting information S3) and are fully consistent with the millennial-scale subsidence map proposed by Grall et al. (2018). Indeed, the craton tends to reduce vertical displacements in its vicinity, whereas weak boundaries amplify them. In some ways, the lithosphere in the delta can be seen as a beam clamped at the west, with a free border at the east, leading to a west-to-east increase of deformation under Holocene sediment loading. This suggests that lateral variability may have strong impact on the regional distribution of subsidence.

Sediment-driven subsidence rates depend on the viscosity of the mantle, as well as the rheology of the plate boundary between India and Eurasia. Although uncertainties remain on their amplitude, subsidence rates of 2–3 mm/year are found to be likely. These values are much larger than those predicted by uniform mantle models where lateral rheological variations were not taken into account (Karpitchev et al., 2018). The discrepancy can be reduced somewhat, however, if an even more diffuse eastern plate boundary is considered. Except for the urban area of Dhaka where much higher rates due to groundwater pumping are reported (Higgins, 2016), sediment isostasy should be thus an important driver of subsidence. It must be underlined, however, that the observed land vertical motions are still expected to differ significantly from the rates of

subsidence estimated in this study, as other drivers can strongly enhance or reduce vertical motions. For example, the core samples collected by Pate et al. (2009) from a borehole near the town of Raipur (10 km east of the Meghna) indicate a rather slow subsidence rate of about 0.5 mm/year. As the core is located on top of an anticline (one of the buried folds of the fold belt), it can therefore be assumed that in this region, the sediment-driven enhanced subsidence is at least partly compensated by active uplift. Sediment compaction is also expected to play a major role, even if its contribution might be more moderate than in other deltas, as sedimentation in the GBMD is dominated by silty-sandy deposits, with relatively low clay content (Grall et al., 2018).

The findings of this study have potentially strong implications for development in the GBMD. First, because the maximum of sediment-driven subsidence is located in the area where the population density is the highest (Figure 5). Although tectonic uplift in the active Indo-Burman ranges to the east limits the impact of subsidence on the population, this may not be the case for the people living close to the plate boundary, especially west of it.

Second, because the response of the Earth to sediment loading is a long-term process with timescales of hundreds to thousands of years. Part of the delta will thus keep sinking irrespectively of human activities. In these regions, a constant supply of sediments is therefore needed to compensate sediment-driven subsidence. This aspect needs to be taken into account in projects currently under study, which might have a considerable impact on sediment transport in the GBMD (Higgins et al., 2018).

Third, long-term subsidence rates of a few millimeters per year in a specific area might have a feedback effect on the location of rivers. One may wonder, for instance, if the late Holocene avulsion of the Ganges eastward could not be at least partially due to the response of the Earth to sediment loading. Changing the course of large rivers can have extremely strong implications for the evolution of a delta, as it results in new sediment starved areas that are prone to erosion and relative sea level rise.

The delta communities are facing major challenges due to increasing uncertainties caused by global changes, including climate change, rapidly growing populations, and increase of human activities impacting well beings of river basins and natural resources. Our findings demonstrate that subsidence driven by sediment loading is one of the important processes contributing to relative sea level rise in the GBMD. Further work is required, however, to better constrain the amplitude of this mechanism (and differentiate the contribution of the various drivers of subsidence) by acquiring additional modern land motion observations. Such effort is indispensable for designing sustainable development strategies in the GBMD.

Acknowledgments

This work was funded by the Belmont Forum/IGFA, G8, Band-Aid project (<http://Belmont-BandAid.org>, funded by ANR in France, by DFG in Germany, and by NSF in the U.S. via Grant ICER-1342644). The NSF program EAR 17-14892 and Lamont-Doherty Earth Observatory are acknowledged for Celine Grall salary support. M. Becker was supported by the French research agency (Agence Nationale de la Recherche, ANR) under the DELTA project (ANR-17-CE03-0001). Data are available through the Open Science Framework (<https://osf.io/mav7h/>).

References

- Blanchon, P., & Shaw, J. (1995). Reef drowning during the last deglaciation: Evidence for catastrophic sea-level rise and ice-sheet collapse. *Geology*, 23(1), 4–8. [https://doi.org/10.1130/0091-7613\(1995\)023<0004:RDDTLD>2.3.CO;2](https://doi.org/10.1130/0091-7613(1995)023<0004:RDDTLD>2.3.CO;2)
- Brammer, H. (1996). *The geography of the soils of Bangladesh*, (p. 287). Dhaka, Bangladesh: University Press, Ltd.
- Broadus, J., Milliman, J. D., Edwards, S. F., Aubrey, D. G., & Gable, F. (1986). Rising sea level and damming of rivers: Possible effects in Egypt and Bangladesh. In J. G. Titus (Ed.), *Effects of changes in stratospheric ozone and global climate* (Vol. 4, pp. 165–189). Washington DC: Environment Protection Agency.
- Brown, S., & Nicholls, R. J. (2015). Subsidence and human influences in mega deltas: The case of the Ganges-Brahmaputra-Meghna. *Science of the Total Environment*, 527–528, 362–374. <https://doi.org/10.1016/j.scitotenv.2015.04.124>
- Chiu, S., & Small, C. (2016). Observations of cyclone-induced storm surge in coastal Bangladesh. *Journal of Coastal Research*, 32, 1149–1161. <https://doi.org/10.2112/JCOASTRES>
- Dziewonski, A. M., & Anderson, D. L. (1981). Preliminary reference Earth model. *Physics of the Earth and Planetary Interiors*, 25(4), 297–356. [https://doi.org/10.1016/0031-9201\(81\)90046-7](https://doi.org/10.1016/0031-9201(81)90046-7)
- Ferrier, K. L., Mitrovica, J. X., Giosan, L., & Clift, P. D. (2015). Sea-level responses to erosion and deposition of sediment in the Indus River basin and the Arabian Sea. *Earth and Planetary Science Letters*, 416, 12–20. <https://doi.org/10.1016/j.epsl.2015.01.026>
- Goodbred, S. L., & Kuehl, S. A. (2000a). Enormous Ganges-Brahmaputra sediment discharge during strengthened early Holocene monsoon. *Geology*, 28(12), 1083–1086. [https://doi.org/10.1130/0091-7613\(2000\)28<1083:EGSDDS>2.0.CO;2](https://doi.org/10.1130/0091-7613(2000)28<1083:EGSDDS>2.0.CO;2)
- Goodbred, S. L., & Kuehl, S. A. (2000b). The significance of large sediment supply, active tectonism, and eustasy on margin sequence development: Late Quaternary stratigraphy and evolution of the Ganges-Brahmaputra delta. *Sedimentary Geology*, 133(3–4), 227–248. [https://doi.org/10.1016/S0037-0738\(00\)00041-5](https://doi.org/10.1016/S0037-0738(00)00041-5)
- Grall, C., Steckler, M. S., Pickering, J. L., Goodbred, S., Sincavage, R., Paola, C., et al. (2018). A base-level stratigraphic approach to determining Holocene subsidence of the Ganges-Meghna-Brahmaputra Delta plain. *Earth and Planetary Science Letters*, 499, 23–36. <https://doi.org/10.1016/j.epsl.2018.07.008>
- Hammer, P., Berthet, T., Hetényi, G., Cattin, R., Drukpa, D., Chopel, J., et al. (2013). Flexure of the India Plate underneath the Bhutan Himalaya. *American Geophysical Union*, 40(16), 4225–4230. <https://doi.org/10.1002/grl.50793>
- Higgins, S. A. (2016). Review: Advances in delta-subsidence research using satellite methods. *Hydrogeology Journal*, 24(3), 587–600. <https://doi.org/10.1007/s10040-015-1330-6>

- Higgins, S. A., Overeem, I., Rogers, K. G., & Kalina, E. A. (2018). River linking in India: Downstream impacts on water discharge and suspended sediment transport to deltas. *Elementa: Science of the Anthropocene (Washington, DC)*, 6(1), 20. <https://doi.org/10.1525/elementa.269>
- Higgins, S. A., Overeem, I., Steckler, M. S., Syvitski, J. P. M., Seeber, L., & Akhter, S. H. (2014). InSAR measurements of compaction and subsidence in the Ganges-Brahmaputra Delta, Bangladesh. *Journal of Geophysical Research: Earth Surface*, 119, 1768–1781. <https://doi.org/10.1002/2014JF003117>
- Hoque, M., & Alam, M. (1997). Subsidence in the lower deltaic areas of Bangladesh. *Marine Geodesy*, 20(1), 105–120. <https://doi.org/10.1080/01490419709388098>
- Ivins, E. R., Dokka, R. K., & Blom, R. G. (2007). Post-glacial sediment load and subsidence in coastal Louisiana. *Geophysical Research Letters*, 34, L16303. <https://doi.org/10.1029/2007GL030003>
- Karpychev, M., & Fleitout, L. (2000). Long-wavelength geoid: The effect of continental roots and lithosphere thickness variations. *Geophysical Journal International*, 143(3), 945–963. <https://doi.org/10.1046/j.1365-246X.2000.00309.x>
- Karpychev, M., Ballu, V., Krien, Y., Becker, M., Goodbred, S., Spada, G., et al. (2018). Contributions of a strengthened early Holocene monsoon and sediment loading to present-day subsidence of the Ganges-Brahmaputra Delta. *Geophysical Research Letters*, 45, 1433–1442. <https://doi.org/10.1002/2017GL076388>
- Krien, Y., & Fleitout, L. (2008). Gravity above subduction zones and forces controlling plate motions. *Journal of Geophysical Research*, 113, B09407. <https://doi.org/10.1029/2007JB005270>
- Latychev, K., Mitrovica, J. X., Tamisiea, M. E., Tromp, J., & Moucha, R. (2005). Influence of lithospheric thickness variations on 3-D crustal velocities due to glacial isostatic adjustment. *Geophysical Research Letters*, 32, L01304. <https://doi.org/10.1029/2004GL021454>
- Li, C., van der Hilst, R. D., Meltzer, A. S., & Engdahl, E. R. (2008). Subduction of the Indian lithosphere beneath the Tibetan Plateau and Burma. *Earth and Planetary Science Letters*, 274(1-2), 157–168. <https://doi.org/10.1016/j.epsl.2008.07.016>
- Milliman, J. D., Broadus, J. M., & Gable, F. (1989). Environmental and economic implications of rising sea level and subsiding deltas: The Nile and Bengal Examples. *Ambio*, 18, 340–345.
- Pate, R. S., Goodbred Jr., S. L., & Khan, S. R. (2009). Delta double-stack: Juxtaposed Holocene and Pleistocene sequences from the Bengal Basin, Bangladesh. *The Sedimentary Record*, 7, 4–9.
- Peltier, W. R. (1974). The impulse response of a Maxwell Earth. *Reviews of Geophysics*, 12(4), 649–669. <https://doi.org/10.1029/RG012i004p00649>
- Rashid, T., Suzuki, S., Sato, H., Monsur, M. H., & Saha, S. K. (2013). Relative sea-level changes during the Holocene in Bangladesh. *Journal of Asian Earth Sciences*, 64, 136–150. <https://doi.org/10.1016/j.jseae.2012.12.007>
- Spada, G., Antonioli, A., Cianetti, S., & Giunchi, C. (2006). Glacial isostatic adjustment and relative sea level changes: The role of lithospheric and upper mantle heterogeneities in a 3-D spherical Earth. *Geophysical Journal International*, 165(2), 692–702. <https://doi.org/10.1111/j.1365-246X.2006.02969.x>
- Steckler, M. S., Akhter, S. H., & Seeber, L. (2008). Collision of the Ganges-Brahmaputra Delta with the Burma Arc: Implications for earthquake hazard. *Earth and Planetary Science Letters*, 273(3-4), 367–378. <https://doi.org/10.1016/j.epsl.2008.07.009>
- Steckler, M. S., Mondal, D. R., Akhter, S. H., Seeber, L., Feng, L., Gale, J., et al. (2016). Locked and loading megathrust linked to active subduction beneath the Indo-Burman Ranges. *Nature Geoscience*, 9(8), 615–618. <https://doi.org/10.1038/ngeo2760>
- Steckler, M. S., Mondal, D.R., Nooner, S.L., Akhter, S.H., Seeber, L., Bettadpur, S.V., et al. (2013). GPS velocity field in Bangladesh: Delta subsidence, seasonal water loading and shortening across the Burma Accretionary Prism, Poster presented at the 2013 Fall Meeting of the AGU, San Francisco, Calif., 9–12 Dec 2013, Abstract T13D-2566.
- Steckler, M. S., Nooner, S. L., Akhter, S. H., Chowdhury, S. K., Bettadpur, S., Seeber, L., & Kogan, M. G. (2010). Modeling Earth deformation from monsoonal flooding in Bangladesh using hydrographic, GPS, and Gravity Recovery and Climate Experiment (GRACE) data. *Journal of Geophysical Research*, 115, B08407. <https://doi.org/10.1029/2009JB007018>
- Syvitski, J. P. M., Kettner, A. J., Overeem, I., Hutton, E. W. H., Hannon, M. T., Brakenridge, G. R., et al. (2009). Sinking deltas due to human activities. *Nature Geoscience*, 2(10), 681–686. <https://doi.org/10.1038/ngeo629>
- Tackley, P. (2000). Self-consistent generation of tectonic plates in time-dependent, three-dimensional mantle convection simulations: 2. Strain weakening and asthenosphere. *Geochemistry, Geophysics, Geosystems*, 1(8). <https://doi.org/10.1029/2000GC000036>
- Wolstencroft, M., Shen, Z., Törnqvist, T. E., Milne, G. A., & Kulp, M. (2014). Understanding subsidence in the Mississippi Delta region due to sediment, ice, and ocean loading: Insights from geophysical modeling. *Journal of Geophysical Research: Solid Earth*, 119, 3838–3856. <https://doi.org/10.1002/2013JB010928>
- WorldPop (2017). India 100 m population, version: 2. University of Southampton. DOI: <https://doi.org/10.5258/SOTON/WP00532>.
- Zhong, S. J., Gurnis, M., & Moresi, L. (1998). Role of faults, nonlinear rheology, and viscosity structure in generating plates from instantaneous mantle flow models. *Journal of Geophysical Research*, 103(B7), 15,255–15,268. <https://doi.org/10.1029/98JB00605>